Indian Journal of Radio & Space Physics
Vol 45, June 2016, pp. 57-66

Triple band ultra-thin metamaterial absorber with wide incident angle stability

D Sood* & C C Tripathi

University Institute of Engineering & Technology, Kurukshetra University, Kurukshetra 136 119, Haryana, India

Received 14 March 2016; revised 26 May 2016; accepted 07 June 2016

In this paper, a triple band electric field driven LC (ELC) resonator based metamaterial absorber with wide incident angle stability has been presented. The design consists of three ELC resonators and dimensions of each are optimized in such a way that absorption is observed at three distinct frequencies covering C, X and Ku-bands to serve potential RF applications. The proposed absorber design provides absorptivity of 66.88%, 98.06% and 99.97% at 4.97, 11.27 and 13.43 GHz, respectively under normal incidence. The absorber structure shows high absorptivity for oblique incidence angles up to 60°. The proposed absorber design has also been studied for various angles of TE polarization under normal incidence. The absorber structure provides the flexibility to adjust each of absorption frequencies separately. An array of the proposed absorber design has been fabricated and its performance is experimentally investigated under normal and oblique incidences for TE polarization. The measured results are observed to be in agreement with the simulation response.

Keywords: Metamaterial absorber, Triple band absorber, ELC resonator design, Ultra-thin metamaterial absorber

PACS No: 84.40.Ba

1 Introduction

An ideal electromagnetic absorber is a device, which absorbs all incident radiations with zero reflection and transmission[1]. The traditional electromagnetic absorbers, like Salisbury screen[2], Jaumann absorbers[3], Dallenbach layers[4] are narrow band and thicker. Therefore, the requirement of electrically thin electromagnetic absorbers with improved bandwidth performance has attracted the attention of researchers towards the metamaterials due to their unusual electromagnetic properties at the sub-wavelength scale[5].The extraordinary properties of metamaterials have been theoretically verified by postulating an artificial engineered structure[6]. Based on this theoretical investigation, the existence of first artificial material with negative effective permittivity and permeability has been experimentally demonstrated[7]. These artificially engineered periodic metamaterial structures can attain their properties from a basic unit cell and have potential applications in cloaking[8], imaging[9], antennas[10], solar cell[11] and perfect absorbers[12]. In a metamaterial based absorber, the size, shape and orientation of the unit cell are engineered to tailor the effective permittivity and permeability of the structure in such a way that when an incident wave falls on it, the input impedance becomes equal to the free space impedance, thereby, causing strong absorption.

*Corresponding author (E-mail: deepaksood.uiet@gmail.com)

Since the development of the first perfect metamaterial absorber[12], efforts have been put by the researchers to improve the performance of metamaterial based absorbers in terms of polarization and incident angle insensitivity[13,14], bandwidth enhancement[15] and ultra-thin thickness[16], etc. The ideas of performance improvement in a metamaterial absorber through polarization and incident angle insensitivity have been suggested[13]. Further, initial ideas of the performance improvement through dual and multiband metamaterial absorber designs for various applications have been reported[17–19]. Till now, various metamaterial based triple band absorber designs have been proposed[20–26]. The absorber presented by Li *et al.*[19] has a complex design and it does not support separate control of absorption frequencies. The absorber designs proposed by Bhattacharya *et al.*[21,22] and Wang *et al.*[23] have larger unit cell size and variations in their physical dimensions do not provide much flexibility for the individual adjustment of the three resonance frequencies, which limits their practical use. Another method to achieve triple band absorption is based on the use of multilayer structure[24]. Although the design is polarization insensitive, the extra fabrication steps and the alignment of multiple layers are the major limitations in such absorber structures. It is also observed that in most of the already proposed absorber designs[22–26], the triple bands are

not obtained in the true sense as out of three absorption frequencies, the two frequencies are generally obtained in a single band such as either C or X-bands. Therefore, the ultrathin metamaterial absorbers, for multiband operations over wide incident angles with flexible design configuration to achieve control of individual frequencies, are still required.

In this paper, an ultra-thin ELC based triple band metamaterial absorber for wide incident angles has been presented. The proposed absorber structure exhibits three absorption peaks in C, X and Ku-band. The performance of the absorber design has been investigated through the illustration of the wide incident angle stability for TE polarization. The field and surface current distributions have been studied to understand the absorption mechanism. The contributions of the individual ELC resonator elements in the proposed absorber design have been studied to investigate the origin of three absorption peaks. Further, the control of absorption frequencies through the variations in dimensions of individual ELC resonators has been demonstrated, which proves that the proposed absorber is a potential candidate to serve various RF applications, such as stealth technology with RCS reduction, photo-detector, bolometer and electromagnetic interference. A prototype array of the proposed absorber design has been fabricated and its performance is experimentally verified under normal and oblique incidences for TE and TM polarizations.

2 Unit Cell Design

The unit cell design of the proposed triple band metamaterial absorber structure is shown in Fig. 1. It consists of three ELC resonator structures in such a manner that two small size ELC resonator structures of different widths are perpendicularly embedded in a large sized ELC resonator. The electric field, magnetic field and wave propagation directions are along X-axis, Y-axis and Z-axis, respectively. The periodicity of the unit cell is 10 mm, which is 0.44 λ correspoding to the highest frequency of absorption, i.e. 13.43 GHz and the structure is designed on a 1.6 mm thick grounded dielectric substrate. The bottom layer is completely metalized. The top and bottom metal layers are made up of copper ($\sigma = 5.8 \times 10^7$ S m^{-1}) of 0.035 mm thickness. The dielectric used is FR4 with electric permittivity $\varepsilon_r = 4.4$ and loss tangent, i.e. tan $\delta = 0.02$. The optimized dimensions of the unit cell are: P = 10 mm, L = 8.5 mm, L_1= 5.0 mm, W_1 = 0.5 mm, W_2 = 0.7 mm, W_3 = 0.5 mm, W_4 = 2.0 mm, g_1 = 0.3 mm, g_2 = 0.3 mm and g_3 = 0.75 mm. The overall thickness of the design is λ/14 corresponding to the highest frequency of absorption. The absorption is evaluated as: $A = 1-|S_{21}|^2 - |S_{11}|^2$. Here, $|S_{21}|^2$ and $|S_{11}|^2$ are transmitted and reflected power, respectively. As the structure is completely copper plated, there is no transmission of power and therefore, $|S_{21}|^2 = 0$. Thus, the absorption can be calculated as: $A = 1 - |S_{11}|^2$.

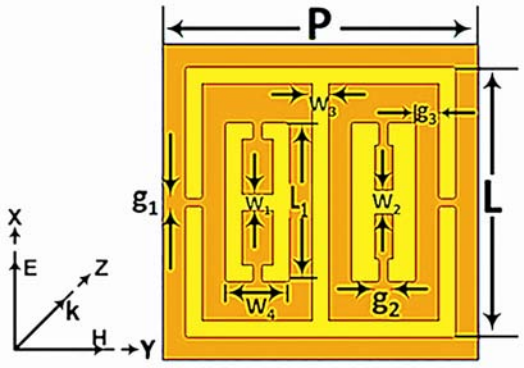

Fig. 1 — Unit cell design of the proposed triple band metamaterial absorber

3 Simulation

The proposed absorber design is simulated by applying Floquet's periodic boundary conditions using Ansys HFSS. The simulated response under normal incidence for TE polarization is shown in Fig. 2. Three absorption peaks (f_1, f_2, and f_3) at 4.97, 11.27 and 13.43 GHz with 66.88, 98.06 and 99.97% absorptivities, respectively has been observed.

3.1 Simulated response of the triple band absorber under different polarization angles

The absorber structure has been studied for various angles of TE polarization under normal incidence as

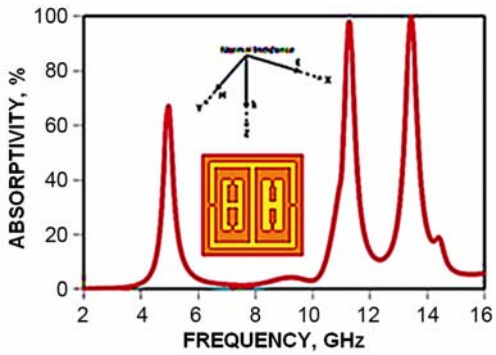

Fig. 2 — Simulated absorptivity response under normal incidence

shown in Fig. 3 and it is noticed that the design shows polarization insensitivity up to 'ϕ' equals to 60°. In TE polarization, the electric field is maintained along X-axis, but the magnetic field changes its direction with respect to Y and Z-axis. At 'ϕ' equals to 90°, the first and second absorption peaks are absent but the third absorption peak is present with minor deviation in frequency.

The performance of the absorber structure has also been investigated for oblique angles of incidence for TE and TM polarizations. The simulated absorptivity for different incidence angles (θ) for TE polarization has been shown in Fig. 4. It is observed that the absorber provides wide angle absorptivity and the absorption peaks remains almost unaltered with the variation in incidence angles. As the design is twofold symmetric, therefore, the similar performance of the proposed absorber has been noticed for different incidence angles (θ) for TM polarization as shown in Fig. 5. Thus, the proposed absorber structure provides wide angle stability with respect to the incident electromagnetic wave. It is also observed that with the increase in incident angle, the absorptivity at the first absorption frequency (f_1) increases. At an incident angle of 60°, the simulated value of absorptivity at 'f_1' has been observed as 85.53%.

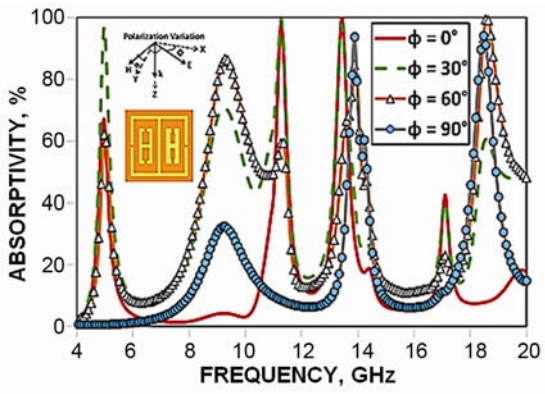

Fig. 3 — Simulated response of the triple band absorber for different angles of polarization under normal incidence

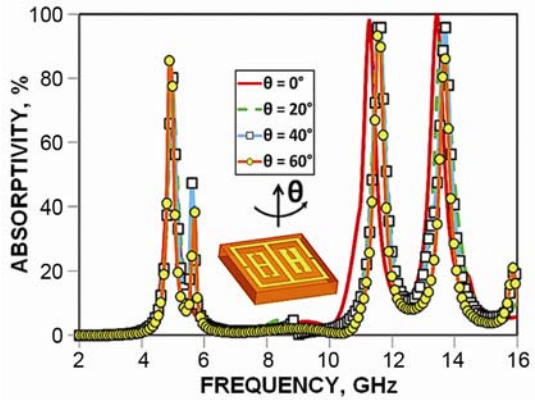

Fig. 4 — Simulated response of the triple band absorber for different incidence angles under TE polarization

4 Absorption Mechanism

For better physical insight of the absorption in the proposed absorber structure, the field and surface current distributions have been examined. The electric and magnetic field distributions for the three absorption frequencies are shown in Fig. 6. It is observed that the first absorption frequency (f_1) is provided by the outer ELC resonator, as at 4.97 GHz, the electric and magnetic fields are primarily distributed at the outer ELC resonator as shown in Figs 6 (a and b). The second absorption frequency (f_2) is mainly occurring due to right side embedded ELC as evident from the field distribution across it, as shown in Figs 6 (c and d). The electric field is capacitive coupled across the gap in the ELC structure; while the magnetic field is inductively coupled along the middle arm of ELC. This electromagnetic coupling provides a strong absorption peak at 11.27 GHz. On the other hand, at the third absorption frequency (f_3) of 13.43 GHz, although the magnetic field is mainly coupled with right side embedded ELC resonator, but the electric field is coupled with left side embedded ELC; thereby, provides electric excitation, which therefore, supports the strong absorption.

The surface current distribution at the three absorption frequencies has also been studied as shown in Fig. 7. From Figs 7 (a and b), it is observed that at (f_1) 4.97 GHz, the current density is higher at the outer ELC resonator and the direction of current is

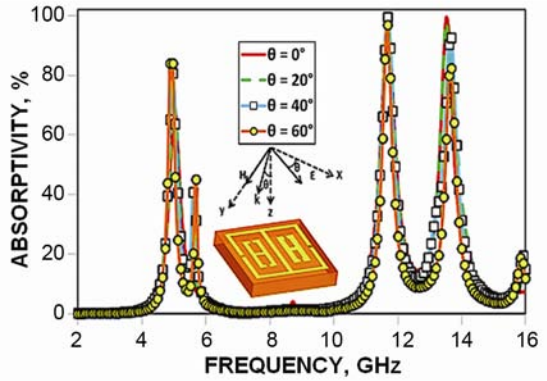

Fig. 5 — Simulated response of the triple band absorber for different incidence angles under TM polarization

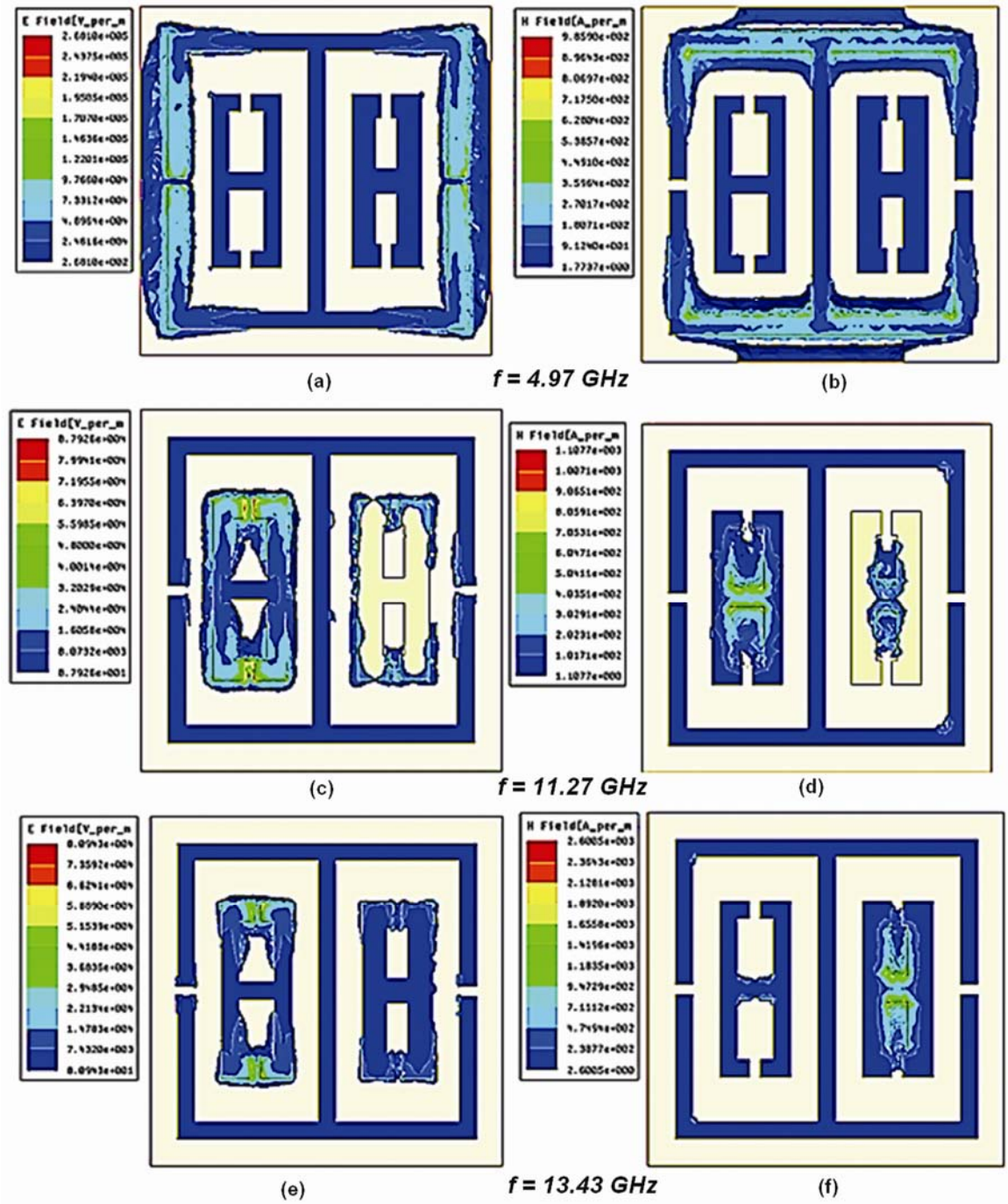

Fig. 6 — Field distribution: (a) electric field and (b) magnetic field at 4.97 GHz; (c) electric field and (d) magnetic field at 11.27 GHz; and (e) electric fieldand (f) magnetic field at 13.43 GHz

antiparallel at the top and bottom layer. At the second absorption frequency (f_2), the surface current mainly distributed along the middle arm of right side embedded ELC resonator, which signifies its contribution in absorption at this frequency as shown in Figs 7 (c and d). Similarly, at the third absorption frequency (f_3), the surface currents are mainly distributed on the left side embedded ELC resonator as evident from the Figs 7 (e and f). For all the three absorption frequencies, the surface currents are antiparallel at the top and bottom surfaces, which generate the circular flow of currents perpendicular to the incident magnetic field, thereby, causing strong magnetic resonance.

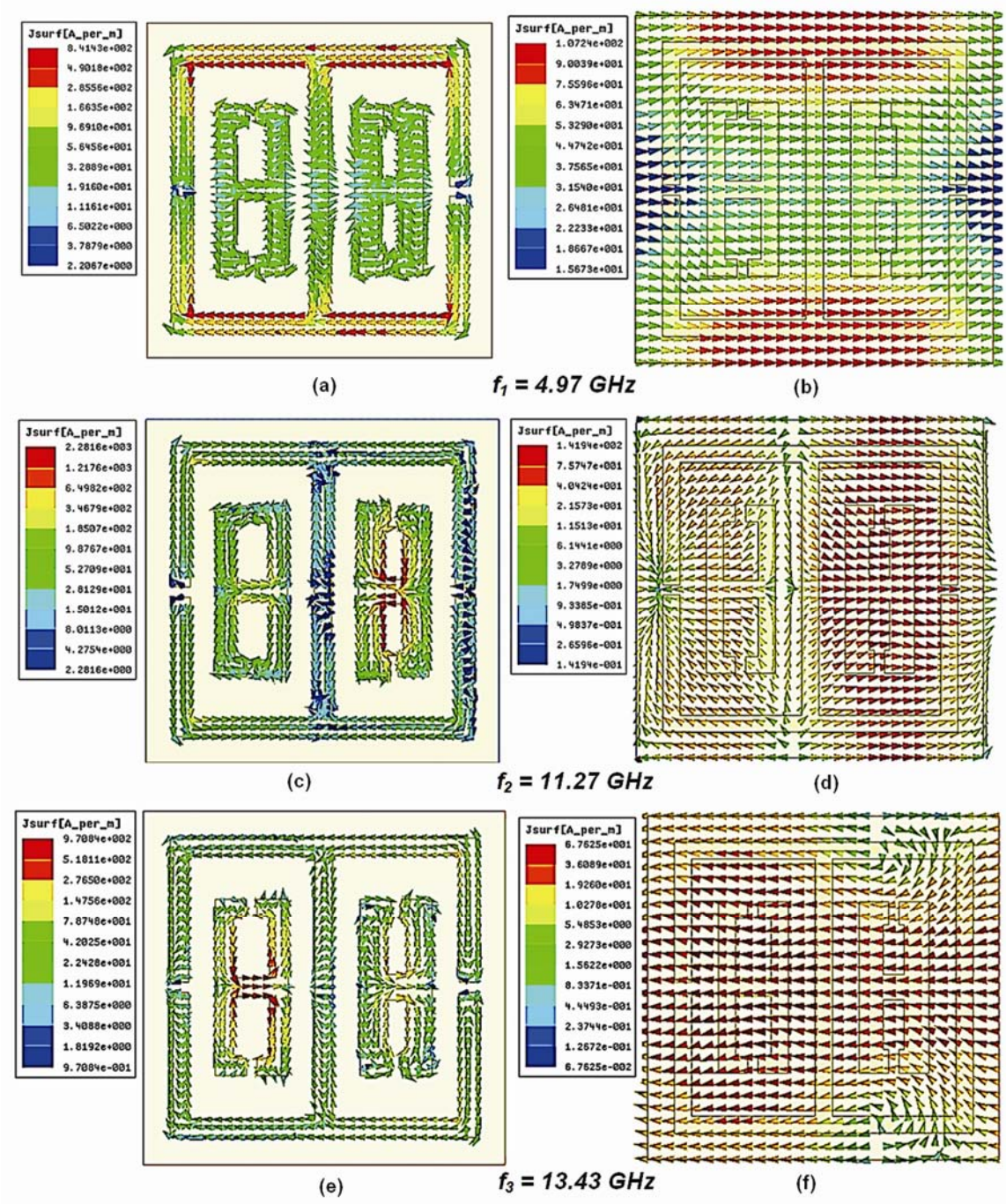

Fig. 7 — Surface current distribution: (a) top and (b) bottom at 4.97 GHz; (c) top and (d) bottom at 11.27 GHz; and (e) top and (f) bottom at 13.43 GHz

Further, in order to understand the enhancement of absorption for oblique incident angles at the lower absorption frequency of 4.97 GHz, the electric and magnetic vector fields for the incident angles of 0° and 60° have been investigated as shown in Fig. 8. The distribution of electric field is observed to be almost same with the increase in incident angle of the electromagnetic wave as shown in Figs 8 (a and b). However, as the incident angle increases to 60°, the magnetic field is observed to be strongly coupled to the outer ELC resonator in comparison to at 0° as shown in Figs 8 (c and d). Thus, the increase in

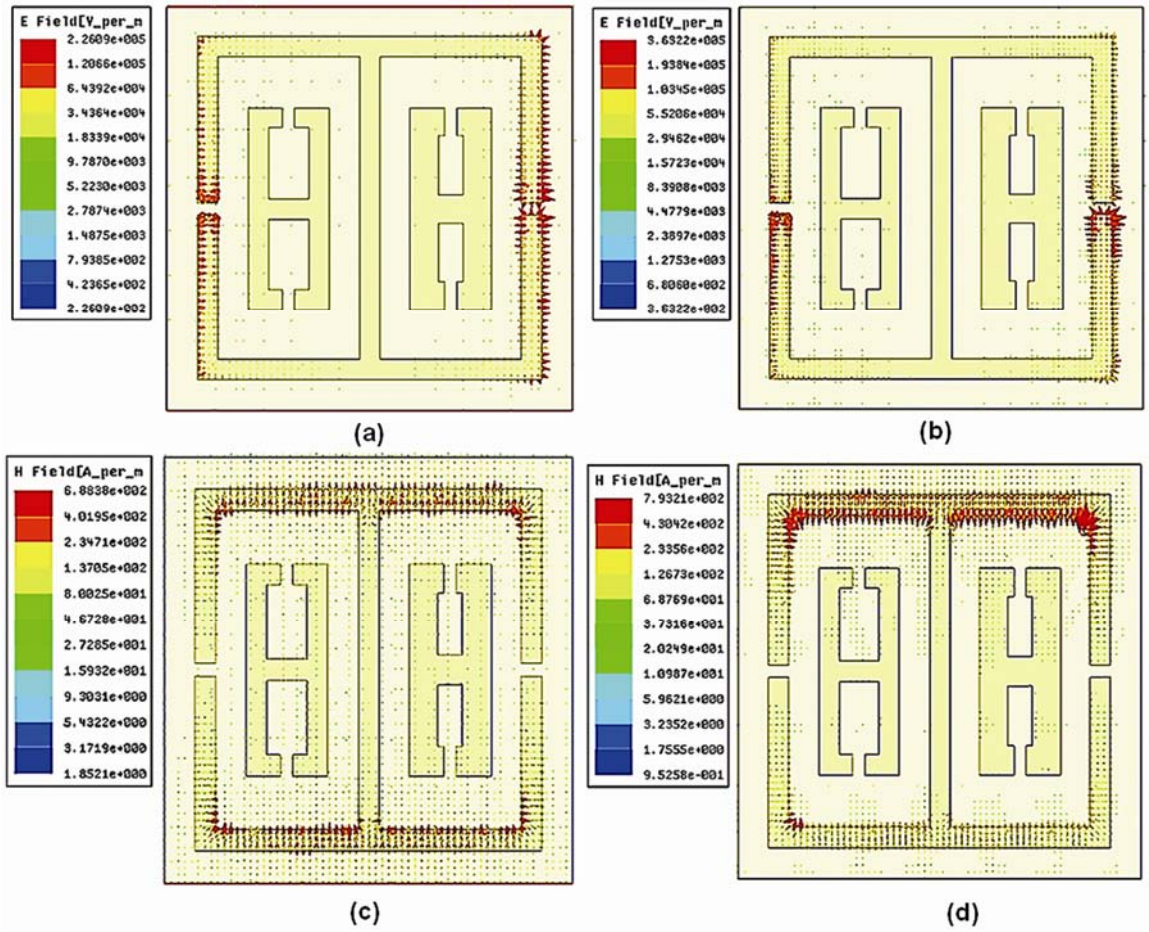

Fig. 8 — E-field vector at 4.97 GHz for: (a) θ = 0° and (b) θ = 60°; H–Field vector at 4.97 GHz for: (c) θ = 0° and (d) θ = 60°.

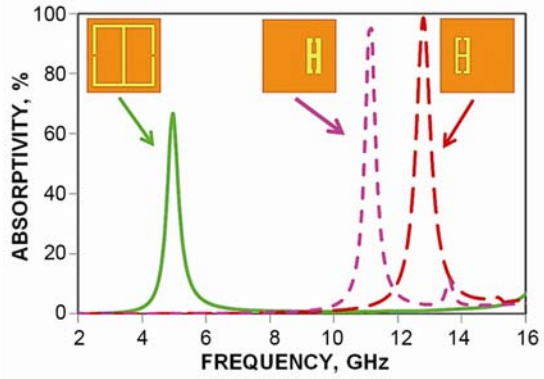

Fig. 9 — Absorption peaks contributed by the individual ELC resonators

magnetic field coupling at the outer ELC resonatorfor oblique incident angles is mainly responsible for the enhancement of absorption.

Thereafter, in order to investigate the origin of three absorption peaks the contribution of the individual ELC resonators has been investigated as shown in Fig. 9. It is observed that the outer ELC resonator provides the first absorption peak at 4.97 GHz, whereas the inner embedded ELC resonators at the right and left side provides the absorption peaks at 11.27 and 13.43 GHz, respectively. Therefore, the three absorption frequencies are separately controlled by the dimensions of the three ELC resonators. This feature provides the flexibility to adjust the absorption frequencies as per requirements for the three distinct microwave bands, i.e. C, X and Ku- bands.

Further, to investigate the independent control of the absorption frequencies, the effects of dimensions of individual ELC structures on the absorption peaks have been studied. For this purpose, dimensions L_1 and W_1 of the left side inner ELC structure have been varied at regular intervals (the same is valid for the right side ELC resonator) as listed in Table 1. It is observed that with the increase in W_1 corresponding to fixed L_1, the third absorption frequency (f_3) increases and the remaining two, i.e. the first and second absorption frequencies remain unaltered. It is also

Table 1 — Shifting of the third absorption frequency (f_3) with variations in dimensions of left side inner ELC resonator

S No	L_1, mm	W_1, mm	f_3, GHz	Absorptivity, %
1	3	0.3	12.80	98.74
2		0.5	14.42	96.80
3		0.7	16.76	81.02
4	5	0.3	9.83	86.10
5		0.5	11.27	98.06
6		0.7	13.43	99.97
7	7	0.3	8.03	74.57
8		0.5	9.02	90.50
9		0.7	10.19	97.08

Table 2 — Variation of first absorption frequency (f_1) with different values of L for fixed W (0.5 mm)

S No	L, mm	f_1, GHz	Absorptivity, %
1	8.5	4.97	66.88
2	7.5	6.14	61.53
3	6.5	7.40	56.16
4	5.5	8.93	51.82

Table 3 — Variation of first absorption frequency (f_1) for different values of W with L fixed at 8.5 mm

S No	W, mm	f_1, GHz	Absorptivity, %
1	0.3	5.06	71.22
2	0.5	4.97	66.88
3	0.7	4.88	40.71

observed that the increase in L_1 from 3 mm to 7 mm for the fixed value of W_1 (0.5 mm), the absorption frequency changes from 14.42 GHz to 9.02 GHz with more than 90% absorptivity. This proves the flexibility of independent controlling of absorption frequencies in the proposed design corresponding to the dimensions of the individual ELC resonators.

Similarly, the effects of dimensional parameters of the outer ELC resonator have been studied. The variation of absorption frequency (f_1) with respect to the dimensions L and W of the outer loop is listed in Tables 2 and 3. It is observed from Table 2 that with the increase in L for a fixed value of width W (0.5 mm), the absorption frequency (f_1) shifts from C band to X-band, thus providing the flexibility to control the first absorption frequency with the other two absorption frequencies (f_2 and f_3) remaining unchanged. On the other hand, for a fixed value of L (8.5 mm), the absorption frequency (f_1) and absorptivity both reduces with the increase in width ’

5 Experimental Verification

For experimental verification of the proposed triple band metamaterial absorber, a prototype array consisting of 15 × 15 unit cells has been fabricated on a 1.6 mm thick FR-4 dielectric substrate as shown in Fig. 10. Measurements of the fabricated prototype have been performed as per the method suggested by Bhattacharya *et al.*[21,22]. The measurement setup, as shown in Fig. 11, consists of two UWB horn antennas (VSWR < 2 for 1 to 18 GHz) connected to Agilent’s vector network analyzer (N5222A) with a frequency range of 10 MHz - 26.5 GHz. One horn antenna acts as a transmitting antenna and the other is used as receiving antenna.

In order to calibrate the test environment, initially a copper sheet of identical dimension has been placed in front of the horn antennas at a distance at which near field effects are negligible. At first, the reflected power from the copper sheet is measured as a reference value. Thereafter, the reflected power for normal incidence has been measured by replacing the

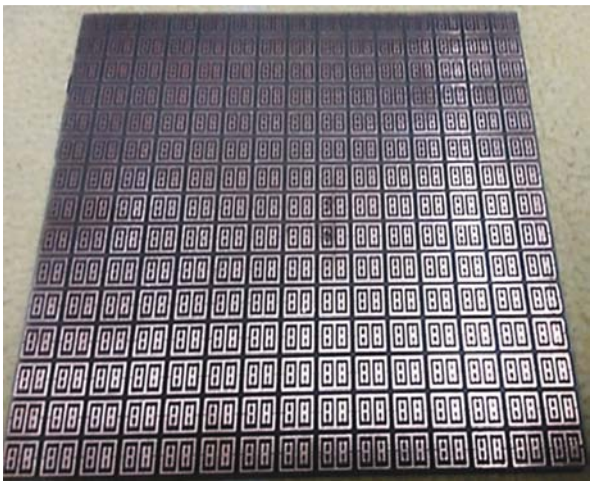

Fig. 10 — Fabricated prototype of triple band metamaterial absorber

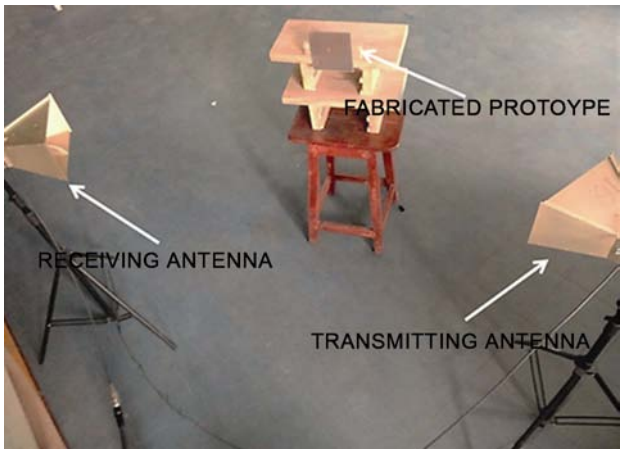

Fig. 11 — Measurement steup (during absorption mesurement for oblique angles of incidence wave)

copper sheet with the fabricated prototype. The difference between these two reflected powers provides the actual reflection of the fabricated structure. The difference between the reflected power nullifies all the scattering, path and diffraction losses as these losses remain same during the measurements of reflected power from copper sheet as well as from fabricated design. Then, the absorption (*A*) is calculated as discussed above. The fabricated structure is supported on a polarization insensitive wooden arrangement in order to have negligible effect on measurements.

The comparison of measured and simulated response under normal incidence is shown in Fig. 12. The measured response provides three absorption peaks at 4.64, 11.44, and 13.61 GHz with absorption values of 64.90, 97.37 and 99.73%, respectively. The percentage errors between the simulated and measured values for the three absorption frequencies are 6.6, 1.5 and 1.3%, respectively.

The fabricated structure has also been experimentally verified for different angles of polarization (ϕ) under normal incidence. For this purpose, the fabricated absorber structure has been rotated about an axis normal to its surface at regular intervals of 30° starting from 0° to 90°. The measured results are shown in Fig. 13. At an angle (ϕ = 60°), the three simulated absorption peaks are observed at 4.97, 11.36 and 13.88 GHz, respectively; while the measured absorptionpeaks are observed at 5.04, 11.52 and 13.92 GHz, respectively. Therefore, simulated and measured absorptivity peaks at ϕ = 60° are quite closer and the proposed absorber provides polarization insensitivity upto an angle of 60°. Further, the performance of the proposed absorber

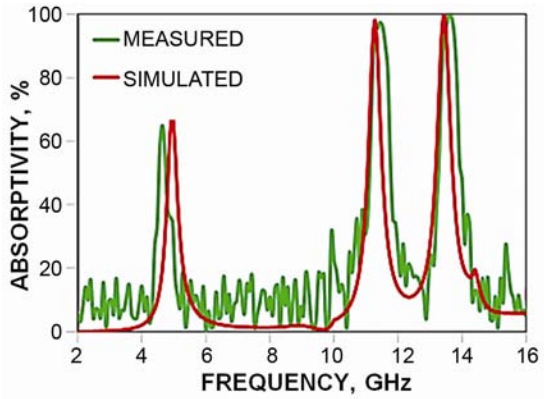

Fig. 12 — Comparison of measured and simulated response of triple band metamaterial absorber under normal incidence for TE polarization

design has been experimentally investigated for oblique incidence angles (θ) of the incoming wave for TE polarization. In this case, the fabricated sample is kept fixed and the UWB horn antennas are rotated at regular intervals of 20° starting from 0° to 60°, along the circumference of a circle at the center of which the fabricated sample is placed and the radius of the circle is equal to the distance at which near field effects are minimized.

The measured results for different angles of incidence of incoming electromagnetic wave for TE polarizationas are shown in Fig. 14. It is observed that the proposed absorber provides wide angle stability with high absorptivity for the incident wave at oblique angles. The fabricated structure is further experimentally tested under oblique incidence for TM polarized wave as shown in Fig. 15. For TM polarization, horn antennas are placed in such a way that magnetic field is aligned in Y direction while the propagation direction and incident electric field vary with an angle θ w.r.t X and Z directions, respectively.

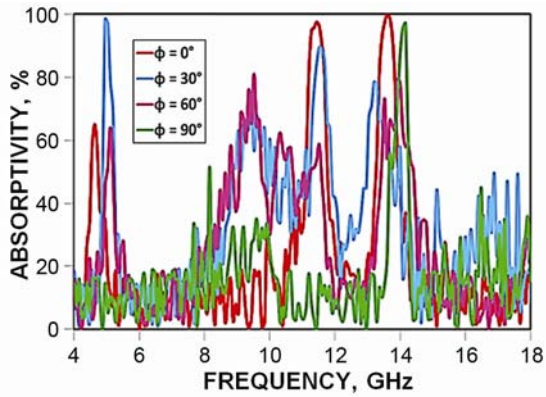

Fig. 13 — Measured results of triple band metamaterial absorber for: (a) different polarization angles (ϕ) of the incident wave under normal incidence

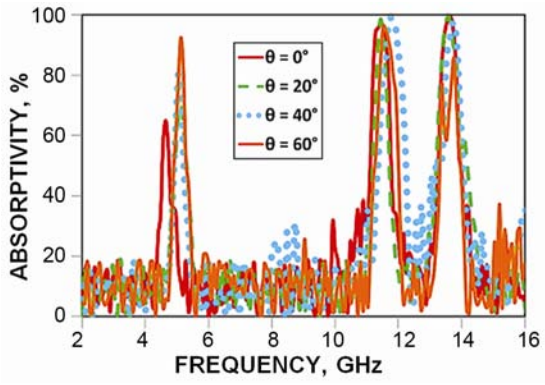

Fig. 14 — Measured results of triple band metamaterial absorber for different angles of incidence (θ) wave with TE polarization

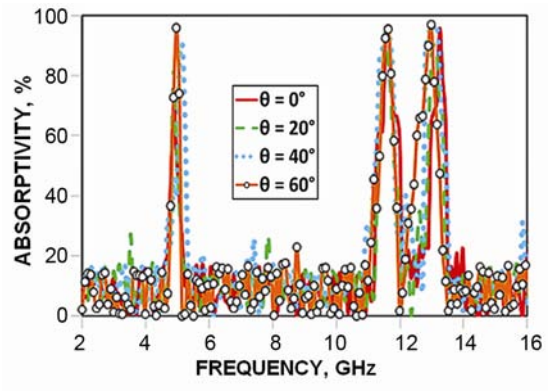

Fig. 15 — Measured results of triple band metamaterial absorber for different angles of incidence (θ) wave with TM polarization

Thus, it is evident that the proposed absorber is angularly stable for the incident angle of incoming electromagnetic wave up to 60°.

6 Conclusions

In this paper, a novel ELC based triple band metamaterial absorber with high absorption at wide incident angles has been proposed. The unit cell design consists of two orthogonally placed ELC resonator structures within a comparatively large sized ELC resonator. The proposed absorber is ultra-thin with its thickness of ~λ/14 corresponding to its highest frequency of absorption. The simulated results show three absorption peaks at 4.97, 11.27 and 13.43 GHz with 66.88, 98.06 and 99.97% absorption rates corresponding to each ELC resonator. Therefore, the proposed design provides the flexibility of independent adjustment of absorption frequencies for different operating bands by optimizing the dimensions of the individual ELC resonator. Here, the geometric dimensions are optimized to serve C, X and Ku-band applications, such as RCS reduction, photo-detector, bolometer and electromagnetic interference. The physical mechanism of absorption has been studied through field and surface current distributions. The experimental verifications for normal and different oblique incidence angles for TE polarization have been performed by testing the fabricated prototype array of the proposed structure. The simulated and experimental results are in agreement. It is observed that the proposed absorber provides wide incidence angle stability with high absorptivity for TE polarization.

Acknowledgement

The work was supported by funding of TEQIP-II (subcomponent 1.1) project for graduate studies and research. The authors are thankful to Mr Saptarshi Ghosh, Ph D Scholar, IIT Kanpur, India for his valuable suggestions in experimental measurements.

References

1 Padilla W J & Liu X, Perfect electromagnetic absorbers from microwave to optical, *SPIE Newsroom (USA)*, 14 Oct (2010).
2 Salisbury W W, Absorbent body of electromagnetic waves, *U S Patent 2,599,944*, June 10 (1952).
3 Ruck G T, Barrick D E & Stuart W D, *Radar cross section handbook*, (Plenum, New York), 1970.
4 Chambers B & Tennant A, Active Dallenbach radar absorber, *in IEEE International Symposium on Antennas and Propagation*, (Albuquerque, New Mexico, USA), 2006, pp 381-384.
5 Veselago V G & Labedev P N, The electrodynamics of substances with simultaneously negative values of ε and μ, *Sov Phys Usp*, 10 (1968) pp 509-514.
6 Pendry J B, Holden A J, Robbins D J & Stewart W J, Magnetism from conductors and enhanced nonlinear phenomena, *IEEE Trans Microwave Theory Tech (USA)*, 47 (1999) pp 2075-2084.
7 Smith D R, Padilla W J, Vier D C, Nemat-Nasser S C & Schultz S, Composite medium with simultaneously negative permeability and permittivity, *Phys Rev Lett (USA)*, 84 (2000) pp 4184.
8 Cummer S A, Popa B I, Schurig D, Smith D R & Pendry J B, Full wave simulations of electromagnetic cloaking structures, *Phys Rev Lett (USA)*, 74 (2006) pp 036621.
9 Fallahi A, Yahaghi A, Benedickter H R, Abiri H,Sarabandi M & Hafner C, Thin wideband radar absorbers, *IEEE Trans Antennas Propag (USA)*, 58 (2010) pp 4051–4058.
10 Ziolkowski R W & Erentok A, Metamaterial-based efficient electrically small antennas, *IEEE Trans Antennas Propag (USA)*, 54 (2006) pp 2113.
11 Hao J, Wang J, Liu X, Padilla W J, Zhou L & Qiu M, High performance optical absorber based on a plasmonic metamaterial, *Appl Phys Lett (USA)*, 96 (2010) pp 251104.
12 Landy N I, Sajuyigbe S, Mock J J, Smith D R& Padilla W J, A perfect metamaterial absorber, *Phys Rev Lett (USA)*, 100 (2008) pp 207402.
13 Luukkonen O, Costa F, Simovski C R, Monorchio A & Tretyakov S A, A thin electromagnetic absorber for wide incidence angles and both polarizations, *IEEE Trans Antennas Propag (USA)*, 57 (2009) pp 3119-3125.
14 Ye Q, Liu Y, Lin H, Li M &Yang H, Multi-band metamaterial absorber made of multi-gap SRRs structure, *Appl Phys A (USA)*, 107 (2012) pp 155-160.
15 Lee J & Lim S, Bandwidth-enhanced and polarisation-insensitive metamaterial absorber using double resonance, *Electron Lett (UK)*, 47 (2011) pp 8–9.
16 Shen X, Cui T J, Zhao J, Ma H F, Jiang W X & Li H, Polarization-independent wide-angle triple-band metamaterial absorber, *Optics Express (USA)*, 19 (2011) pp 9401-9407.
17 Wen Q Y, Zhang H W, Xie Y S, Yang Q H & Liu Y L, Dual band terahertz metamaterial absorber: design, fabrication and characterization *Appl Phys Lett (USA)*, 95 (2009) pp 241111.
18 Tao H, Bingham C M, Pilon D, Fan K, Strikwerda A C, Shrekenhamer D, Padilla W J, Zhang X & Averitt R D, A dual band terahertz metamaterial absorber, *J Phys D (UK)*, 43 (2010) pp 225102.

19 Li H, Yuan L H, Zhou B, Shen X P & Cheng Q, Ultrathin multiband gigahertz metamaterial absorbers, *J Appl Phys (USA)*, 110 (2011) pp 014909.

20 Xu H X, Wang G M, Qi M Q, Liang J G, Gong J Q, & Xu Z M, Triple-band polarization-insensitive wide-angle ultra-miniature metamaterial transmission line absorber, *Phys Rev B (USA)*, 86 (2012) pp 205104.

21 Bhattacharyya S, Ghosh S &Srivastava K V, Triple band polarization-independent metamaterial absorber with bandwidth enhancement at X-band, *J Appl Phys (USA)*, 114 (2013) pp 094514.

22 Bhattacharyya S & Srivastava K V, Triple band polarization-independent ultra-thin metamaterial absorber using electric field-driven LC resonator, *J Appl Phys (USA)*, 115 (2014) pp 064508.

23 Wang G D, Chen J F, Hu X W, Chen Z Q & Liu M H, Polarization-insensitive triple-band microwave metamaterial absorber based on rotated square rings, *Prog Electromagn Res (USA)*, 145 (2014) pp 175–183.

24 Huang L & Chen H, Multi-band and polarization insensitive metamaterial abso, *Prog Electromagn Res (USA)*, 113 (2011) pp 103-110.

25 Ayop O, Rahim M K A, Murad N A, Samsuri N A & Dewan R, Triple Band Circular Ring-Shaped Metamaterial Absorber for X-Band Applications, *Prog Electromagn Res M (USA)*, 39 (2014) pp 65–75.

26 Zhai H, Zhan C, Li Z & Liang C, Triple-band ultrathin metamaterial absorber with wide-angle and polarization stability, *IEEE Antennas Wireless Propag Lett (USA)*, 14 (2015) pp 241–244.